# System Scaling Approach and Thermoeconomic Analysis of a Pressure Retarded Osmosis System for Power Production with Hypersaline Draw Solution: A Great Salt Lake Case Study

Thomas T.D. Tran, Keunhan Park, Amanda D. Smith*

*Department of Mechanical Engineering, University of Utah, Salt Lake City, UT 84112*

**Abstract**

Osmotic power with pressure retarded osmosis (PRO) is an emerging renewable energy option for locations where fresh water and salt water mix. Energy can be recovered from the salinity gradient between the solutions. This study provides a comprehensive feasibility analysis for a PRO power plant in a hypersaline environment. A sensitivity analysis investigates the effects of key technical and financial parameters on energy and economic performances. A case study is developed for the Great Salt Lake in Utah, USA (which has an average 24% salt concentration). A 25 MW PRO power plant is investigated to analyze the necessary components and their performances. With currently available technologies, the power plant would require 1.54 $m^3/s$ (24,410 GPM) fresh water flow rate and 3.08 $m^3/s$ (48,820 GPM) salt water flow rate. The net annual energy production is projected to be 154,249 MWh, with capital cost of $238.0 million, and operations and maintenance cost of $35.5 million per year. The levelized cost of electricity (LCOE) would be $0.2025/kWh, but further design improvements would reduce the LCOE to $0.1034/kWh. The high salinity of the Great Salt Lake is a critical factor toward making the osmotic power plant economically feasible.

*Keywords:* pressure retarded osmosis, power generation, renewable energy, hydroelectric, levelized cost

## 1. Introduction

Renewable energy is a growing portion of the power generation sector. Compared to traditional power generation methods, the benefits of generating power from renewable energy sources include the reduction in greenhouse gas emissions. Pressure retarded osmosis (PRO) makes use of energy recovery from a salinity gradient between two bodies of water. Figure 2 illustrates the schematic of the PRO process. The higher saline solution is called the draw solution while the lower saline solution is referred to as the feed solution. Semipermeable

*Site-Specific Energy Systems Laboratory

*Email address:* amanda.d.smith@utah.edu (Amanda D. Smith)

membranes, which only allow fresh water to pass through while preventing salt water from permeating, are placed between the two solutions. Electric power then can be recovered as the permeate solution is run through a hydroturbine. Practical PRO systems are most suitable for locations with fresh water and saline water sources nearby. For example, river-to-sea or river-to-hypersaline-lake sites can become potential locations for future PRO power plants.

Recent PRO studies have mostly focused on investigating PRO performance with bench-scale systems. Membrane behaviors and influence of operating conditions toward PRO performance have been studied with bench-scale systems and commercially available membranes [1, 2, 3]. In bench-scale studies, the use of forward osmosis (FO) membranes in PRO applications introduces the possibility of membrane rupture. This is due to the fact that FO membranes are not designed to withstand high hydraulic pressure in PRO experiments. Mesh spacers within PRO membrane housings have been introduced as an effective solution for this problem. Hickenbottom et al. investigated different mesh spacers configuration to achieve higher PRO performance [4]. The presence of mesh spacers provides membranes with better mechanical support and longer operation, although they affect the water flux across the membrane [3, 4].

Improving membranes for PRO applications has naturally become a next step in the development of PRO power generation technology. Several membrane modification methods have been utilized to alter membrane structure. Among all, interfacial polymerization is the most widely used method, especially with thin film composite (TFC) FO membranes [5]. The advantage of using interfacial polymerization can be shown by the flexibility to individually tailor and optimize the structure and properties. As a result, desired permeability coefficients can be achieved and concentration polarization is reduced [5]. Modified TFC membranes for PRO experiments have been tested to performance better than typical TFC membranes under the same conditions [6, 7].

Osmotic pressure is also an important factor in PRO performance. Due to the difference in salt concentration, water tends to flow from the feed solution to the draw solution. The osmotic pressure is defined as the pressure that should be applied to the draw solution to stop the osmotic water flow [8]. Experimental studies of bench-scale PRO systems with higher osmotic pressure yielded higher power density compared to similar experiments with lower osmotic pressure [1, 4, 9]. As a result, local sites providing higher osmotic pressure difference between the feed solution and the draw solution can potentially generate more electric power. The Great Salt Lake in Utah, USA has been identified for its high salinity, ranging from 6% to 27% [10]. To put this in perspective, the average salinity of seawater is 3.5%. The saltiest natural water source in the world is the Dead Sea with an average salt concentration of 33.7% [8]. In addition to the high saline water, the Great Salt Lake is also located near fresh water sources such as the Bear, Weber, and Jordan Rivers. The Great Salt Lake has been identified as a possible location for future implementation of PRO in power generation, given the availability of high saline draw solution and fresh water supplies.

In this study, a practical 25 MW PRO system is investigated by considering the Great Salt Lake as a potential location. The interactions between system components are investigated and integrated into a system-level model. The results from this study test the

feasibility of a PRO power generation implementation with currently available technology, and an economic analysis is presented incorporating a number of technical costs. A sensitivity analysis is used to identify the relative impacts of specific parameters in the model. Furthermore, recommendations are provided for reducing cost in an effective way toward enhancing PRO's competitiveness with other renewable technology. The results from this study can increase understanding of large-scale PRO systems and inform decision making for those interested in future PRO implementations.

## 2. Osmotic Power with PRO

### *2.1. PRO Power Density*

In PRO, the power density is used to define the power that can be obtained per unit area of membrane. The ideal power density of PRO is described by:

$$W = J_w \Delta P = A(\Delta\pi - \Delta P)\Delta P \tag{1}$$

where $W$ (W/m$^2$) is the power density, $J_w$ (m$^3$/m$^2 \cdot$ s) is the water flux, $A$ (m/s $\cdot$ kPa) is the water permeability coefficient, $\Delta\pi$ (kPa) is the osmotic pressure difference, and $\Delta P$ (kPa) is the hydraulic pressure difference.

However, Eq. (1) does not consider the concentration polarization across the membrane. Concentration polarization is a type of membrane fouling which produces a concentration gradient, particle build-up near the membrane, and reduced available surface area. McCutcheon et al. showed that concentration polarization has adverse impacts on the performance of PRO [11]. There are two types of concentration polarization: internal concentration polarization (ICP) and external concentration polarization (ECP). ECP happens when salt is collected on the external side of the membrane while ICP is due to the accumulation of salt inside the support layer of the membrane [11]. By considering the concentration polarization, the power density equation in PRO can be modified as [1, 8, 12]:

$$W = A\left[\pi_{D,b} exp(-\frac{J_w}{k})\frac{1 - \frac{\pi_{F,b}}{\pi_{D,b}} exp(J_w K) exp(\frac{J_w}{k})}{1 + \frac{B}{J_w}\left[exp(J_w K) - 1\right]} - \Delta P\right]\Delta P \tag{2}$$

where $\pi_{D,b}$ (kPa) is bulk osmotic pressure in the draw solution, $\pi_{F,b}$ (kPa) is bulk osmotic pressure in the feed solution, $B$ (m/s) is the salt permeability coefficient, $k$ (m/s) is external concentration polarization mass transfer, and $K$ (m/s) is internal concentration polarization mass transfer coefficient.

### *2.2. Annual Energy Production*

Annual energy production from a PRO power plant can be calculated from the expected level of power generation and the number of hours that the power plant is operated. As a result, the annual produced energy equation is:

$$E_{production} = \dot{W}_{net} \times CF \times t \tag{3}$$

where $E_{production}$ (MWh) is the annual energy production, $\dot{W}_{net}$ (MW) is the power capacity of the power plant, $CF$ is the capacity factor, and $t$ (hour) is the number of hours in a year.

*2.3. Gibbs Free Energy of Mixing*

The osmotic energy in PRO can be derived from the Gibbs free energy of mixing, which occurs when two solutions with different compositions are mixed. In a reversible PRO process, the maximum extractable work is equal to the Gibbs free energy of mixing [13]:

$$\frac{\Delta G}{iRT} = \frac{c_{final}}{\phi} \ln c_{final} - c_{fs} \ln c_{fs} - \frac{1-\phi}{\phi} c_{ds} \ln c_{ds} \tag{4}$$

where $\Delta G$ (or $E_{osmotic}$) (kWh/m$^3$ of fresh water) is the mixing energy per unit volume of fresh water. Initial feed solution concentration, initial draw solution concentration, and final solution concentration are represented by $c_{fs}$ (mol/L or M), $c_{ds}$ (mol/L or M), and $c_{final}$ (mol/L or M), respectively. Furthermore, $\phi$ is the ratio of the initial volume of the feed solution to the initial total volume of both the feed and draw solutions, $R$ (L $\cdot$ kPa/mol $\cdot$ K) is the universal gas constant, $T$ (K) is the absolute temperature, and $i$ is the number of osmotically active particles in the solution. The Gibbs free energy of mixing is maximum when the ratio of the initial volume of the feed solution to the total initial volume approaches zero. Calculation of a river-to-sea PRO system reveals the maximum mixing energy to be 0.81 kWh/m$^3$ of fresh water [13]. However, the actual specific energy should be lower than the maximum theoretical value due to irreversibilities and system inefficiencies [13, 14, 15].

*2.4. Solution Flow Rate through the Power Plant*

With the osmotic energy and the power generation, the required flow rate of the fresh water through the power plant can be found by the following equation:

$$Q_{fs} = \frac{\dot{W}_{net}}{E_{osmotic} \times 3.6} \tag{5}$$

where $Q_{fs}$ (m$^3$/s) is the flow rate of the fresh water and 3.6 is a unit conversion factor between $\dot{W}_{net}$ (MW) and $E_{osmotic}$ (kWh/m$^3$) to get $Q_{fs}$ (m$^3$/s). About 90% of the fresh water will eventually be able to permeate through the membrane while the other 10% of the fresh water can be recycled [16]. Regarding the flow rate of the salt water, it is recommended that the ratio of the salt water to the fresh water is 2 to 1 in order to optimize the performance of the system [17, 18]. The salt water flow rate is calculated below:

$$Q_{ds} = 2 \times Q_{fs} \tag{6}$$

where $Q_{ds}$ (m$^3$/s) is the flow rate of the salt water. With the intake flow rates of the fresh water and the salt water, the brackish water (the mixed solution of the fresh and salt waters) outfall flow rate can be obtained by the following equation:

$$Q_{bs} = 0.9 \times Q_{fs} + 2.0 \times Q_{fs} = 2.9 \times Q_{fs} \tag{7}$$

where $Q_{bs}$ (m$^3$/s) is the flow rate of the brackish water and 0.9 accounts for 90% of the permeated fresh water.

## 3. Bench-scale PRO Systems

### *3.1. Design of Experimental Setup*

A typical bench-scale PRO system can be broken down into 2 subsystems: the membrane housing and solutions intake. Figure 3 illustrates the schematic of a typical bench-scale PRO system. Membrane housing is the most important component in a PRO bench-scale setup. The design of membrane housing is similar among recent studies [1, 3, 4]. Symmetric channels on both sides of the membrane housing allow the feed and draw solutions flow tangential to the membrane surface. Fresh water in bench-scale PRO systems is usually deionized water or concentration-controlled fresh water. Salt water is prepared by mixing sodium chloride with deionized water. The concentration of the draw solution can be controlled by the amount of sodium chloride in DI water. This flexibility allows PRO studies with different combinations of feed solution and draw solution concentrations.

### *3.2. Membrane Performance in PRO*

Membranes in PRO applications require high mechanical strength to withstand a hydraulic pressure applied from the draw solution side. In the early days of PRO development, reverse osmosis (RO) membranes were selected because of their ability to tolerate high pressure [19, 20]. However, using RO membranes yielded low power densities [19, 21]. The thick supporting layer of RO membranes is undesirable in PRO process since it holds back the free diffusion of molecules and reduces the effective osmotic pressure across the membrane [12]. This particular design of RO membrane structure increases ICP and decreases PRO performance.

After unsuccessful attempts with RO membranes, FO membranes have been utilized in PRO experiments. FO membranes possesses desirable membrane characteristics such as high water flux and low salt reverse flux [5]. In both FO and PRO processes, the fresh water crosses the semipermeable membrane to the saline water due to the osmotic pressure difference between the two solutions. In theory, commercially available FO membranes can be used in PRO applications. Flat-sheet cellulose triacetate (CTA) and TFC FO membranes are the most investigated FO membranes as reported in the literature [1, 2, 4, 9]. The thin membrane structure allows the CTA and TFC membranes to have higher water flux and lower salt reverse flux. Power densities greater than 5 $W/m^2$ have been achieved in laboratory setups with FO membranes [22, 23].

Even though the performance of FO membranes in PRO experiments has been improved significantly over the last decade, commercially available FO membranes still experience concentration polarization, which significantly reduces their performance [11]. Moreover, current FO membranes are not optimized for the hydraulic pressure from the draw solution in the PRO process. Since FO membranes are generally used in low pressure environments, they are likely to be deformed in high pressure environments. For the PRO process, the characteristics of a high performance membrane are the ability to reject solutes from the draw solution, allow high water transport, and withstand high hydraulic pressure [24].

## 4. Osmotic Power at the Great Salt Lake

The Great Salt Lake has desirable characteristics for potential PRO power plants. As one of the largest and saltiest lakes in the world, the Great Salt Lake is located in a unique situation. The salt concentration in the lake is varied with location and time throughout the year. The lake has no outflow (only through evaporation) and three inflows (the Bear, Weber, and Jordan Rivers). With the construction of the railroad causeway in 1959 to connect the east and the west of the basin, the lake was divided into four distinguished bays (the Gunnison Bay, the Gilbert Bay, the Bear River Bay, and the Farmington Bay) as seen in Fig. 4 [25]. The average salinity in the Bear River Bay and the Farmington Bay is the lowest among the four bays (up to 9%) since the inflow of fresh water from the Bear river and the Jordan river, respectively. The two major bays, the Gunnison Bay and the Gilbert Bay, have much higher salinities. The Gunnison Bay, which is located in the northern part of the Great Salt Lake, has no inflow of fresh water. As a result, the average salinity in the Gunnison Bay is around 30%. On the contrary, the Gilbert Bay receives 90% of the inflow water to the Great Salt Lake. Its average salinity (10% to 18%) is considerably lower than that of the Gunnison Bay [26]. Nonetheless, the salt concentration in the Great Salt Lake is consistently greater than the typical salinity in seawater, which is around 3.5%.

In this study, the salt concentration from the Great Salt Lake is taken as an averaged value of 24% (or 240 g/L). The salt concentration in the fresh solution is considered to be 0.05% (or 0.5 g/L). The theoretical maximum osmotic energy from the Gibbs free energy of mixing of the two solutions is 5.54 kWh/m$^3$ if the volume ratio ($\phi$) approaches zero. When the flow rate ratio of the draw solution to the feed solution is 2 (or $\phi = 0.33$), the osmotic energy is 4.50 kWh/m$^3$, which is about 18.8% less than the maximum osmotic energy. In this study, the following calculation of energy production is based on the more realistic osmotic energy (4.5 kWh/m$^3$ is equivalent to 100% of the total available osmotic energy). Helfer et al. estimated the theoretical power of the Great Salt Lake to be around 400 MW [8]. To put this in perspective, the net electricity generation in Utah in Feb. 2016 was around 2,822 GWh, in which renewable energy accounted for only 162 GWh (about 5.7 % of total net electricity generation) [27]. The electricity supply from the osmotic power can be adequate for 300,000 households [8]. System design integration and cost analysis for a potential PRO power plant at the Great Salt Lake can identify key aspects for building a successful PRO system.

## 5. Design of a Practical 25 MW PRO System

Practical PRO systems are similar to bench-scale PRO systems with the addition of several important components, such as pretreatment for the freshwater and the saltwater, pressure exchanger, turbine, and generator. The practical PRO system in this study consists of these subsystems: membrane module, solution intake and outfall system, solution pre-treatment, and an electro-mechanical power generation system (turbine, generator, pressure exchanger, etc.). Integration of these subsystems are described below in Fig. 5. Furthermore, capital cost, operations and maintenance cost, energy loss, and energy consumption analysis for these subsystems will be investigated.

*5.1. Solution Intake Systems*

The solution intake systems in this PRO system convey solutions from rivers and the Great Salt Lake to the PRO power plant site. The solution intake systems can be varied from system to system, depending on the geographic situation of the power plant site. Solution intake systems should be carefully designed to meet the flow rate demand of the system. Figure 6 shows the schematic diagram of the deep-water intake system. Another important aspect of solution intake systems is to minimize the environmental impacts from diverting the fresh water and the salt water from their original sources. As opposed to shallow water intake, direct deep-water intake is a preferred method for water conveyance since it can provide more uniform water properties and reduce impacts on local ecology [14].

*5.1.1. Capital Cost*

The capital costs for the solution intake systems are the costs for constructing piping and pumping. Depending on the distance of the power plant relative to the fresh and salt water sources, the capital cost of the intake system can make up a large portion of the total capital cost. The equations to calculate capital costs of transporting the fresh water and the salt water to the PRO power plant can be written as:

$$C_{intake,fs} = V_{material,fs} \times C_{unit,c} \tag{8}$$

$$C_{intake,ds} = V_{material,ds} \times C_{unit,c} \tag{9}$$

where $C_{intake,fs}$ (\$) and $C_{intake,ds}$ (\$) are the capital cost of intake systems for the feed solution and the draw solution, respectively. $V_{material,fs}$ ($m^3$) and $V_{material,ds}$ ($m^3$) are the constructing material volumes of the intake systems for the feed solution and the draw solution, respectively. The constructing material volumes are dependent on the cross sectional area and the length of the intake systems. $C_{unit,c}$ (\$/$m^3$) is the unit price for building 1 $m^3$ of the water intake system with necessary materials and components.

*5.1.2. Net Annual Energy Consumption*

The solution intake systems for PRO will also require energy input for pumping demands. The annual energy for solution intake systems can be calculated using the energy consumption for pumps. The energy required to transport the feed and draw solutions is described below:

$$E_{i,fs} = \frac{\rho_{fs} \times g \times H_{fs} \times Q_{fs} \times t \times CF}{\eta_{pump} \times 10^6} \tag{10}$$

$$E_{i,ds} = \frac{\rho_{ds} \times g \times H_{ds} \times Q_{ds} \times t \times CF}{\eta_{pump} \times 10^6} \tag{11}$$

where $E_{i,fs}$ (MWh) is the annual energy consumption of pumps for the feed solution, $\rho_{fs}$ (kg/$m^3$) is the density of the fresh water, $H_{fs}$ (m) is the head of the fresh water, $\eta_{pump}$ is the efficiency of pumps, and $10^6$ is to convert Wh to MWh. The efficiency for low-head and high-flow pumps is considered to be 75% [28]. The energy consumption for conveying the draw solution in Eq. (11) is similar to Eq. (10) with the correct density, flow rate, and head for the draw solution.

*5.2. Solution Pre-treatment*

The solution pre-treatment is an important subsystem in this PRO power plant due to impurities from the incoming solutions. The primary metric to determine the quality of the solutions is water turbidity, which is designed to measure the relative clarity of water. In PRO, the maximum acceptable turbidity is 0.5 nephelometric turbidity units (NTU) [29]. Membrane fouling happens when impurities from the feed and draw solutions are accumulated on the membrane. The process of cleaning these impurities is costly and interrupts power generation. In some cases, removing of impurities is irreversible. As a result of membrane fouling, the overall efficiency of the PRO power plant will be reduced. Pre-treatment for solutions is essential to ensure the quality of solutions coming to the membrane module and ultimately minimizes membrane fouling. Several filtration methods for solution pre-treatment have been introduced. Among all, micro-filtration is recommended for the fresh water and the salt water [30]. The mechanism of micro-filtration is illustrated in Fig. 7. The pore size of membranes is typically 0.1 to 10 µm in the micro-filtration process [31]. This process will eliminate undesirable particles before the solutions enter the membrane module.

*5.2.1. Capital Cost and Annual Cost*

The cost of the pre-treatment system can be divided into capital cost and annual cost. Implementation of filtration systems (include micro-filtration membrane, pumping, discharging, etc.) for the fresh water and the salt water requires initial investment, which can be estimated by the following equations:

$$C_{f,fs} = Q_{fs} \times C_{unit,f} \times 86,400 \tag{12}$$

$$C_{f,ds} = Q_{ds} \times C_{unit,f} \times 86,400 \tag{13}$$

where $C_{f,fs}$ (\$) is the capital cost of micro-filtration for the feed solution, $C_{f,ds}$ (\$) is the capital cost of micro-filtration for the draw solution, $C_{unit,f}$ (\$/m$^3$) is the unit price of capital cost micro-filtration, and 86,400 is the number of seconds in a day. The capital cost estimation is based on the daily capacity of the micro-filtration process [31]. Equation (12) and (13) take into account the necessary components in the filtration system.

The annual cost of the solution pre-treatment system is associated with the cost of cleaning and replacing micro-filtration membranes. The expected membrane life ($m_{life}$) is to be at least 5 years [32]. The annual cost of solution pre-treatment can be estimated as following:

$$C_{f,fs,O\&M} = Q_{fs} \times C_{unit,f,O\&M} \times 86,400 \times 365 \tag{14}$$

$$C_{f,ds,O\&M} = Q_{ds} \times C_{unit,f,O\&M} \times 86,400 \times 365 \tag{15}$$

where $C_{f,fs,O\&M}$ (\$) is the annual cost of micro-filtration for the feed solution, $C_{f,ds,O\&M}$ (\$) is the annual cost of micro-filtration for the draw solution, and 86,400 is the number of seconds in a day. Furthermore, $C_{unit,f,O\&M}$ (\$/m$^3$) is the unit price of annual cost for micro-filtration. This is estimated based on daily filtration quantity [31]. The annual O&M costs are computed by multiplying the daily cost by the number of days in a year (365 days).

*5.2.2. Net Annual Energy Consumption*

Additionally, the solution pre-treatment subsystem consumes input energy. Equation (16) and (17) estimate the annual energy consumption for filtration.

$$E_{f,fs} = \Delta P_f \times Q_{fs} \times t \times CF \times 10^{-6} \tag{16}$$

$$E_{f,ds} = \Delta P_f \times Q_{ds} \times t \times CF \times 10^{-6} \tag{17}$$

where $E_{f,fs}$ (MWh) is the annual energy consumption of filtration for the feed solution, $E_{f,ds}$ (MWh) is the annual energy consumption of filtration for the draw solution, $\Delta P_f$ (Pa) is the pressure loss during the filtration process, and $10^{-6}$ is to convert Wh to MWh.

*5.3. Membrane Module*

The membrane module in a practical PRO system is one of the most important subsystems in the entire system. The performance of the membrane module can directly influence the overall efficiency of the system. As previously stated, the spiral wound membrane module design is more applicable to practical PRO systems than the flat-sheet membrane module. The packing density of spiral wound membrane module is 775 $m^2/m^3$ [33]. To put this in perspective, it would take a whole soccer field (or football pitch) with flat-sheet membrane to pack 8.25 $m^3$ of spiral wound membrane, given the area of the soccer field is around 6,400 $m^2$ (approximately 68,889 $ft^2$).

The configuration of membrane module design can be varied. O'Toole et al. studied two configurations of membrane modules, parallel membrane module and tiered membrane module [14]. Parallel membrane modules in PRO are similar to those in desalination plants. The feed solution and draw solution are supplied to each module. Contrarily, tiered membrane modules recycle some of the feed solution from the previous membrane module for the next membrane module. This setup reduces the consumption of treated fresh water. Therefore, overall efficiency of the system can be increased [14].

*5.3.1. Capital Cost and Annual Cost*

The capital cost of membrane is proportional to the area of the membrane used in the power plant. The total membrane area needed can be determined from the targeted power capacity of the power plant and the amount of power which can be generated per square meter. The conventionally targeted power density from membranes in PRO is 5 $W/m^2$, which has been reported to be the break-even point for PRO technology [8, 34]. This power density is economically sufficient for river-ocean setups. As stated earlier, the salinity in the Great Salt Lake is 2 to 7 times higher than the typical seawater salinity. In this study, a power density of 5.0 $W/m^2$ is conservatively assumed from the membrane that is used in the power plant. The total membrane area can be calculated from the following equation:

$$A_m = \frac{\dot{W}_{net} \times 10^6}{W} \tag{18}$$

where $A_m$ ($m^2$) is the membrane area and $10^6$ is the conversion factor between $\dot{W}_{net}$ (MW) and $W$ ($W/m^2$) to get $A_m$ ($m^2$). The total capital cost of membrane module can be calculated from the unit price of membrane per $m^2$, which has been estimated to be around $7.5

per $m^2$ [18].

$$C_m = A_m \times C_{unit,m} \tag{19}$$

where $C_m$ (\$) is the capital cost of membrane module and $C_{unit,m}$ (\$/$m^2$) is the unit price of the membrane module.

The annual cost of the membrane module comes from cleaning and replacing existing membranes. Membranes in PRO experiments have not been tested long enough to estimate the expected life. However, with proper cleaning and maintenance, membranes used in PRO can last as long as membranes used for different applications such as desalination [8, 35]. The annual cost of operations and maintenance of the membrane module can be calculated as:

$$C_{m,O\&M} = Q_{fs} \times C_{unit,m,O\&M} \times 86,400 \times 365 \tag{20}$$

where $C_{m,O\&M}$ (\$) is the annual cost of membrane module, $C_{unit,m,O\&M}$ (\$/$m^3$) is the unit price of annual cost membrane module, and 86,400 is the number of seconds in a day. This estimation is based on daily capacity [36]. The annual O&M cost is calculated by multiplying 365 days.

*5.3.2. Net Annual Energy Consumption*

The net annual energy consumed in the membrane module comes from pumping requirements to deliver the feed and the draw solution to the membrane. Equation (21) and (22) describe the net annual energy for membrane module:

$$E_{m,fs} = \frac{\rho_{fs} \times g \times H_m \times Q_{fs} \times t \times CF}{\eta_{pump} \times 10^6} \tag{21}$$

$$E_{m,ds} = \frac{\rho_{ds} \times g \times H_m \times Q_{ds} \times t \times CF}{\eta_{pump} \times 10^6} \tag{22}$$

where $E_{m,fs}$ (MWh) is the annual energy consumption of pumps to deliver the feed solution, $E_{m,ds}$ (MWh) is the annual energy consumption of pumps to deliver the draw solution, $H_m$ (m) is the hydraulic head across the module, and $10^6$ is to convert Wh to MWh.

*5.4. Electro-mechanical Equipment*

Electro-mechanical equipment in the PRO power plant consists of pressure exchangers, turbines, generators, and their associated mechanical components.

*5.4.1. Pressure Exchanger*

Pressure exchangers, which are energy recovery devices, are utilized in the PRO system. Information about pressure exchangers surfaced on conceptual drawings of proposed large-scale PRO system diagrams [8, 37, 38]. The purpose of the pressure exchanger in a PRO system is to deliver pressure from the diluted seawater to the incoming seawater, which ultimately reduces the power consumption [37]. The operation of pressure exchangers is illustrated in Fig. 8. The implementation of pressure exchangers in PRO systems can potentially increase the overall efficiency in the long run, while adding initial cost to the whole system setup.

*5.4.2. Turbine and Generator*

The turbine and generator are necessary components in this practical PRO system. Turbine and generator technologies themselves are very well-developed. As a result, their efficiencies can be achieved over 90% [14]. Based on commercially available turbines and generators, the efficiencies of turbines and generators are considered to be 90% and 95% in this study, respectively. The operations of turbine and generator in PRO are very similar to those used in hydroelectric renewable energy. The permeate solution in PRO is run through the turbine and generator to generate electric power.

*5.4.3. Capital Cost and Annual Cost*

The capital cost of the electro-mechanical system for the PRO power plant is similar to that of hydroelectric power. Aggidis et al. studied the costs of small-scale hydroelectric power plants. The cost of electro-mechanical equipment has been statistically formulated in the following equation [39]:

$$C_{em} = 12,000 \times (\dot{W}_{stack} \times 10^3 / H_m^{0.2})^{0.56} \times n_{stack} \times f \tag{23}$$

where $C_{em}$ (\$) is the capital cost of the electro-mechanical equipment, $\dot{W}_{stack}$ (MW) is the power capacity per stack, $H_m$ (m) is the head, $n_{stack}$ is the number of membrane stacks, and $f$ is the currency converter from £ to \$. In this study, a number of membrane modules are placed in the same pressure vessel, where a number of pressure vessels are stacked in one membrane stack. Each membrane stack can operate independently from other membrane stacks [18]. The membrane modules in the setup are placed in 5 separated membrane stacks.

*5.4.4. Net Annual Energy Consumption*

Energy losses in the turbine and the generator can be derived from the efficiency of each. The energy loss equation for turbines and generators is presented in Eq. (24):

$$E_{turb,loss} + E_{gen,loss} = E_{production} \times (1 - \eta_{turb}) \times (1 - \eta_{gen}) \tag{24}$$

where $E_{turb,loss}$ (MWh) is the energy loss from turbines, $\eta_{turb}$ is the efficiency of turbines, and $\eta_{gen}$ is the efficiency of generators.

*5.5. Brackish Outfall System*

The solution after turbine and generator is called the brackish water, which is returned to the draw solution source. The salt concentration of the brackish water is similar to the salt concentration of mixing original feed solution and draw solution. However, the brackish water might contain undesirable chemicals after passing membrane and other components in the system. Post-treatment for the brackish water is necessary before discharging back to the source. The presence of brackish outfall system will also introduce initial cost and power consumption to the whole system.

*5.5.1. Capital Cost and Annual Cost*

Similar to the capital cost of the solution intake system, the capital cost of the brackish outfall system can be estimated in Eq. (25):

$$C_{outfall,bs} = V_{material,bs} \times C_{unit,d} \tag{25}$$

where $C_{bs}$ (\$) is the capital cost of brackish outfall system, $V_{material,bs}$ ($m^3$) is the constructing material volume for the brackish solution, which is calculated from the cross-sectional area and the length of the outfall system. Moreover, $C_{unit,d}$ (\$/$m^3$) is the unit price of the discharge system to build 1 $m^3$ of the outfall system (including piping and pumping).

*5.5.2. Net Annual Energy Consumption*

The net annual energy consumption from the brackish outfall system comes from the amount of energy required to discharge the brackish solution. Equation (26) details the calculation:

$$E_{o,bs} = \frac{\rho_{bs} \times g \times H_{bs} \times Q_{bs} \times t \times CF}{\eta_{pump} \times 10^6} \tag{26}$$

where $E_{o,bs}$ (MWh) is the annual energy consumption of pumps in the outfall system, $\rho_{bs}$ (kg/$m^3$) is the density of the brackish solution, $H_{bs}$ (m) is the head of the brackish solution, and $10^6$ is to convert Wh to MWh.

*5.6. Previous Practical PRO Systems*

The first PRO prototype power plant was built in 2009 in Tofle, Norway by Statkraft, a Norwegian state-owned power company [8]. Initially, the prototype power plant utilized 2000 $m^2$ of flat sheet FO cellulose acetate membranes in spiral wound modules. The power density with this type of membrane revealed to be only 0.5 $m^2$ [38]. Due to the low power density, FO cellulose acetate membranes were placed by RO thin-film composite membranes in spiral wound modules. The power density was increased to 1.0 $m^2$ [8]. Given the membrane area of the prototype power plant, the power production was around 2 kW. The low power density of RO membrane was largely due to concentration polarization. As mentioned earlier, the thick support in RO membranes is undesirable in PRO applications as it traps more particles, which reduces the water flux across the membrane over time.

## 6. Modeling Results of the PRO Power Plant

*6.1. System Requirements*

In order to meet the power generation requirement for the PRO power plant, the feed solution and the draw solution must be supplied with correct flow rates. As described in the section on Previous Practical PRO Systems, Equations (5) and (6) calculate the flow rate of the incoming solutions. Table 1 lists the flow rate requirement of both solutions, along with the flow rate of the brackish solution that will be discharged from the system.

*6.2. Net Energy Production*

Applying the first Law of Thermodynamics to the whole system, the net annual energy production is equal to annual energy production minus all the energy losses and consumption by various components in the system. The net annual energy is described by the following equation:

$$E_{net} = E_{production} - E_{loss} \tag{27}$$

Table 2 lists important values from the analysis of the power plant. The net energy production is 154,249 MWh with all the major energy losses and consumption taken into account. The high osmotic energy from the Great Salt Lake contributes significantly toward the net energy production. This is one of the benefits of using the hypersaline lake as a source for the draw solution.

Table 3 breaks down the energy loss and consumption for different subsystems. Intake and outfall systems consume about 5% of the potential energy production. This is due to the pumping demand to deliver solutions from their sources to the power plant and to discharge the brackish solution. Furthermore, the electro-mechanical system (pressure exchangers, turbines, generators, etc.) also registers 15% of energy loss due to their inefficiencies. The solution pre-treatment and membrane module also consume a considerable amount of energy, although they are much less than those of the other systems. The total energy loss accounts for about 22% of the potential energy production. As a result, approximately 78% of osmotic energy can be obtained. If the maximum theoretical osmotic energy was considered (when $\phi$ equals to zero), the overall efficiency is around 63%. This high efficiency is again due to the advantage of using high salt concentration draw solution. This number would be much lower if seawater were used as the draw solution.

*6.3. Total Cost of the Power Plant*

The total capital cost of the power plant is calculated based on the following equation:

$$C_{capital} = C_{intake,ds} + C_{intake,fs} + C_{f,ds} + C_{f,fs} + C_m + C_{em} + C_{outfall,bs} + C_{misc} \tag{28}$$

The calculated capital cost of each subsystem is shown in Table 4. All miscellaneous costs (including site preparation, shipping, installation, startup, etc.) are considered in $C_{misc}$, which is assumed to be 3% of the total capital expenditures. These costs are highly uncertain until the site of installation is determined and material selections for the power plant are completed. Each of the cost values in Eq. 28 should be updated at each design phase, from conceptual drawings to installation.

The operations and maintenance cost of the power plant comes from solution pre-treatment and membrane module subsystems. The annual O&M cost is calculated below:

$$C_{O\&M} = C_{f,ds,O\&M} + C_{f,fs,O\&M} + C_{m,O\&M} \tag{29}$$

Additionally, there is a reoccurring O&M cost to replace fouling membranes. This reoccurring cost is estimated to be half of the membrane module capital cost. The annual and reoccurring O&M costs are listed in Table 5 along with the capital cost of the power plant. The annual O&M cost is about 14% of the capital cost.

### *6.4. LCOE of the PRO power plant*

The levelized cost of electricity (LCOE) is a metric to measure the cost of producing electricity. The LCOE can indicate the break-even point of the technology and point out the feasibility of the project from investors' point of view. The LCOE equation is described below:

$$LCOE = \frac{Total\ Lifetime\ Cost}{Total\ Lifetime\ Energy\ Production} = \frac{\sum_{y=1}^{n} \frac{C_{total}}{(1+r)^y}}{\sum_{y=1}^{n} E_{net}} \tag{30}$$

where $C_{total}$ (\$) is the total cost over lifetime, $E_{net}$ (kWh) is the total energy production over lifetime, $r$ (%) is the discount rate, $y$ (year) is the annual time step, and $n$ (year) is the lifetime of the project.

In this analysis, the discount rate is considered to be 2% and the lifetime of the project is 40 years. The system's LCOE is calculated to be \$0.2025/kWh. On the consumer side, local utility Rocky Mountain Power charges an average residential electricity price in Utah of \$0.1071/kWh [40]. These two prices differ by 89.1%. Comparing the system's LCOE of \$0.2025/kWh to the LCOE of other established renewable energy technologies, the number is relatively higher as seen in Table 6. The LCOEs of other renewable energy technologies are taken as average total system LCOE values for plants entering service in 2022 [41].

## 7. Sensitivity Analysis

The sensitivity analysis in this study focuses on the energy performance, system cost, and economics of the PRO power plant. The energy performance sensitivity analysis can identify significant impacts on the net energy production of the system by different components or subsystems. The sensitivity analysis on capital costs will point out the most costly subsystems toward the capital cost of building the power plant. Additionally, external factors (discount rate and investment period) will be considered in the economics sensitivity analysis to illustrate the effects of financial considerations on the system's LCOE. The goal of this sensitivity analysis is to provide guidance for reducing the price of electricity from the PRO power plant.

### *7.1. Energy Performance*

The energy performance of the power plant is studied with variations in efficiencies of the turbine, generator, and pump. Their design values in this study and their ranges are listed in Table 7. These components are chosen because of their significant contributions toward the net energy production of the power plant.

### *7.2. System Cost*

The cost of the power plant mostly depends on the performance of membrane, solution pre-treatment, membrane module, and membrane lifetime. The performance of membrane is associated with the power density obtained from membranes in PRO. Any increasing in

the power density will result in less membrane needed and less material for the membrane module. Similarly, the unit prices of the solution pre-treatment and the membrane module can have significant impacts on the capital cost of the system. Their unit costs can be varied over time, depending on the development of the technology. Furthermore, the lifetime of membrane can determine the cost for membrane replacement. Table 8 details the ranges of these parameters.

### *7.3. Economics*

Besides energy performance and system cost parameters, there are external parameters that could potentially affect the LCOE of the power plant. Investment period and discount rate are investigated in this study. The design values and ranges of values are based on typical values for investment.

### *7.4. Results of Sensitivity Analysis*

The results of the sensitivity analysis on the system cost, energy performance, and levelized cost are reported in Table 10. Changes in the net energy production, system cost, and LCOE are listed in the table to demonstrate the effects of varying these parameters.

Efficiencies of electro-mechanical components have significant impacts on the net energy production. Net energy production is increased considerably with higher efficient components. Figure 9 and 10 detail the changes of net energy production and LCOE by varying turbine and generator efficiencies, respectively. The price of electricity from the power plant can be reduced by \$0.0260/kWh with turbine efficiency increased from 85% to 95%. Similarly, increasing generator efficiency from 90% to 98% reduces the system's LCOE by \$0.0213/kWh. Contrarily, the net energy gain from more efficient pumps in Fig. 11 is relatively small compared to those of turbines and generators. This is due to the fact that energy losses by electro-mechanical systems are much greater than energy losses by pumping.

The trends from the system cost sensitivity analysis are expected. For the solution pre-treatment and the membrane module, lowering these unit prices can lower the capital cost, as seen in Fig. 12 and Fig. 13. The reduction from these subsystems is important since their combined capital cost is more than 50% of the total capital cost. Furthermore, the membrane performance has significant impact on the total capital cost of the power plant. Using high performing membranes can lower the amount of membrane module and membrane materials needed for the power plant. Figure 14 illustrates the change in LCOE and the capital cost with respect to membrane performance in term of $W/m^2$. An LCOE reduction of \$0.1047/kWh can be attained by having membranes with power density increased from 1 to 15 $W/m^2$. Additionally, the rate of reduction in the LCOE and capital cost level off once the power density reaches about 10 $W/m^2$. This observation suggests that increasing the membrane performance is more significant when the power density is increased up to 10 $W/m^2$. Further improvements in power density are not as impactful as initial power density improvements; that is, improvements in power density show diminishing returns in terms of overall system performance improvements. Nonetheless, this sensitivity analysis demonstrates that increasing power density obtained from membranes in PRO systems can

potentially reduce the capital cost of building the power plant. As a result, a significant reduction in the LCOE from the power plant can be achieved.

Moreover, the membrane lifetime can influence the total membrane cost during the power plant lifetime. Longer membrane longevity can reduce the membrane cost, as seen in Fig. 15. It is also worth noticing that the membrane lifetime cost is the same for membrane lifetime of 8 and 9 years. This is due to the fact that the lifetime of the power plant considered is 40 years, which uses the same amount of membranes regardless of membrane lifetime of 8 or 9 years.

Economic factors also have significant impacts on the LCOE of the power plant. Figure 16 shows the changes in the system's LCOE with different investment periods. Increasing in the investment period reduces the LCOE. Increasing the investment period from 30 to 50 years can reduce the LCOE by \$0.0504/kWh. Due to the additional cost from membrane replacement for every 5 years, the plot in Fig. 16 shows periodicity, with a change in the relationship between LCOE and investment period considered at 5-year intervals. Additionally, increasing the discount rate also reduces the LCOE as seen in Fig. 17. The impacts from economic factors on the system's LCOE cannot be underestimated. The results in this section have shown the considerable changes in the LCOE as the economic factors vary.

### *7.5. Improved Design and Its Results*

Based on the results of the sensitivity analysis, the design parameters have been adjusted to develop improved design requirements that will reduce the LCOE to meet the local price for residential electricity purchases. The combined effects of these improvements are presented as follows: In this improved design, the unit price of solution pre-treatment capital cost is reduced to \$250/m$^3$. The unit price of membrane module is \$5/m$^2$. Turbine and generator efficiencies are increased by 3% each. Furthermore, the efficiency of pump is increased to 80%. The investment period is 50 years instead of 40 years. The discount rate is 4.5% instead of 2%. Membrane performance is increased to 10 W/m$^2$. The membrane lifetime is extended to 8 years instead of 5 years. Other design values are kept at their default values. The results of this improved design are presented in Table. 11. With this new setup, the LCOE is calculated to be 0.1034 \$/kWh. The capital cost with the improved design values is \$197.2 million and the net energy production is 166,837 MWh. As with other power generation technologies, the current price of electricity (or "grid parity") can be reached by having more efficient components and reducing capital cost of subsystems.

## 8. Conclusions and Recommendations

In this study, a feasibility analysis was conducted for a 25 MW PRO power plant and the engineering and economic characteristics that influence the plant's potential profitability were investigated. The location for this power plant is at the Great Salt Lake in Utah, USA, a location chosen for its high salinity, which provides a draw solution with high osmotic energy potential. The design of the power plant was based on currently available technology and the effects of specific technical advances were also described.

For the plant to operate with an output power of 25 MW, the flow rates of the fresh water and the salt water have been calculated to be 1.54 $m^3/s$ (24,410 GPM) and 3.08 $m^3/s$ (48,820 GPM), respectively. The net annual energy production from this power plant would be 154,249 MWh. Furthermore, the capital cost is expected to be $238.0 million with annual O&M costs averaging $33.5 million. The membrane replacement cost is 18.8 million per membrane lifetime. The LCOE of $0.2025/kWh results from financial calculations using a 2% discount rate and 40 year investment period. The price of electricity can be reduced to $0.1034/kWh by minimizing capital costs of some components while improving membrane performance and lifetime, increasing component efficiencies, and extending the investment period.

To be economically feasible, the following improvements are recommended for the 25 MW PRO power plant at the Great Salt Lake:

- Reduce the current cost for micro-filtration ($\$275/m^3$ of solution). The cost of the solution pre-treatment is a major contributor toward the capital cost of the power plant.

- Improve membrane performance to increase the power density. Power densities greater than 5 $W/m^2$, a commonly accepted metric for potential profitability, are desirable. As less membrane area is required, fewer membrane modules will be required for power generation and the capital cost for membrane modules will be decreased. Further development in membrane technology for the PRO process is crucial for the success of PRO power generation technology, although performance increases over 10 $W/m^2$ would be not be as impactful.

- Invest in highly efficient system components. Efficiency improvements for components in the electro-mechanical system (particularly the turbine-generator and pressure exchanger) will improve performance for the whole system. Fewer energy losses increase the net energy production from the power plant.

- Use state and federal incentives for renewable power generation and power plant financing where available. As with any renewable power generation technology, government incentives can make osmotic power more economically feasible.

Additionally, the development of osmotic power with PRO cannot be separated from its environmental consequences. Even though the process mimics the natural discharging of water from nearby rivers into the Great Salt Lake, the introduction of electro-mechanical components alters the hydrological process and may alter local ecosystems. As described in the section on Solution Intake Systems, the design of the intake system in deep water was mentioned to minimize this impact. Moreover, the discharge of the brackish solution from the power plant is an environmental concern if there are any chemicals in the solution. A life cycle impacts assessment for the combined systems comprising an osmotic power plant is necessary to understand and mitigate the actual environmental impacts of PRO power plants to the surrounding ecosystems.

Land and water issues would also require careful consideration in the pre-design phase. Any new power plant also has land and permitting requirements. An osmotic power plant

in the Great Salt Lake area would be complicated since it would likely be sited on public land. Water is critical for the operation of this plant, and the water level in the Great Salt Lake and its nearby rivers vary seasonally and from year to year. The availability of the feed and draw solutions will determine whether the power plant can operate as designed. Nonetheless, if the above-mentioned key points are carefully considered in the research and development process, osmotic power with PRO can become an attractive alternative in the power generation mix.

**Acknowledgement**

This work was supported by a University of Utah Research Foundation seed grant, #10033856. Thomas Tran's work was supported by a Global Change and Sustainability Center Fellowship. The authors gratefully acknowledge graduate research student Carlo Bianchi for his assistance.

**Abbreviations**

| | |
|---|---|
| CTA | Cellulose triacetate |
| ECP | External concentration polarization |
| FO | Forward osmosis |
| ICP | Internal concentration polarization |
| LCOE | Levelized cost of electricity |
| O&M | Operations and maintenance |
| PRO | Pressure retarded osmosis |
| RO | Reverse osmosis |
| TFC | Thin film composite |

**Input Values**

| | |
|---|---|
| $\Delta P_f$ | Solution pre-treatment pressure (30,000 Pa) [18] |
| $\eta_{gen}$ | Generator efficiency (95%) |
| $\eta_{pump}$ | Pump efficiency (75%) |
| $\eta_{turb}$ | Turbine efficiency (90%) |
| $\rho_{bs}$ | Density of the brackish solution (1127.7 kg/m$^3$) |
| $\rho_{ds}$ | Density of the draw solution (1191.5 kg/m$^3$) |

| | |
|---|---|
| $\rho_{fs}$ | Density of the feed solution (1000 kg/m$^3$) |
| $\phi$ | Volume ratio (1/3) |
| $V_{material,bs}$ | Volume of piping material for the brackish solution (36.1 $\times$ 10$^3$ m$^3$) |
| $V_{material,ds}$ | Volume of piping material for the draw solution (35.3 $\times$ 10$^3$ m$^3$) |
| $V_{material,fs}$ | Volume of piping material for the feed solution (34.3 $\times$ 10$^3$ m$^3$) |
| $c_{ds}$ | Draw solution concentration (4.11 mol/L) |
| $c_{fs}$ | Feed solution concentration (8.50 $\times$ 10$^{-3}$ mol/L) |
| $CF$ | Capacity factor of the power plant (0.9) |
| $C_{unit,c}$ | Unit price of conveying solution (\$725/m$^3$) [18] |
| $C_{unit,d}$ | Unit price of discharging solution (\$725/m$^3$) [18] |
| $C_{unit,f}$ | Unit price of capital cost for solution pre-treatment (\$275/m$^3$) [31] |
| $C_{unit,f,O\&M}$ | Unit price of annual cost for solution pre-treatment (\$0.08/m$^3$) [31] |
| $C_{unit,m}$ | Unit price of capital cost of membrane module (\$7.5/m$^2$) [18] |
| $C_{unit,m,O\&M}$ | Unit price of annual cost of membrane module (\$0.45/m$^3$) [36] |
| $f$ | Currency converter from £ to \$ (1.25) |
| $g$ | Gravitational acceleration (9.81 m/s$^2$) |
| $H_{bs}$ | Head of the brackish solution (10 m) |
| $H_{ds}$ | Head of the draw solution (10 m) |
| $H_{fs}$ | Head of the feed solution (10 m) |
| $H_m$ | Head of the membrane module (3 m) |
| $i$ | Number of osmotically active particles (2) |
| $n_{stack}$ | Number of membrane stacks (5) |
| $r$ | Discount rate (2%) |
| $R$ | Universal gas constant (8.314 L $\cdot$ kPa/K $\cdot$ mol) |
| $t$ | Number of hours in a year (8760 hours) |
| $T$ | Temperature (298 K) |

| | |
|---|---|
| $W$ | Power density (5 W/m$^2$) |
| $\dot{W}_{net}$ | Power generation of the power plant (25 MW) |
| $\dot{W}_{stack}$ | Power generation per stack (25/5 MW) |

**Nomenclature**

| | |
|---|---|
| $\Delta P$ | Hydraulic pressure difference (kPa) |
| $\Delta G$ | Mixing energy per unit volume of fresh water (kWh/m$^3$) |
| $\pi$ | Osmotic pressure (kPa) |
| $\pi_{D,b}$ | Osmotic pressure of the bulk draw solution (kPa) |
| $\pi_{D,m}$ | Osmotic pressure of the draw solution at the membrane surface (kPa) |
| $\pi_{F,b}$ | Osmotic pressure of the bulk feed solution (kPa) |
| $\pi_{F,m}$ | Osmotic pressure of the feed solution at the membrane surface (kPa) |
| $A$ | Water permeability coefficient (m/s $\cdot$ kPa) |
| $A_m$ | Membrane area (m$^2$) |
| $B$ | Salt permeability coefficient (m/s) |
| $c$ | Molar concentration (mol/L) |
| $c_{final}$ | Final solution concentration (mol/L) |
| $C_{capital}$ | Capital cost (million dollars) |
| $C_{em}$ | Capital cost of electro-mechanical system ($) |
| $C_{f,ds}$ | Draw solution pre-treatment capital cost ($) |
| $C_{f,ds,O\&M}$ | Draw solution pre-treatment annual cost ($) |
| $C_{f,fs}$ | Feed solution pre-treatment capital cost ($) |
| $C_{f,fs,O\&M}$ | Feed solution pre-treatment annual cost ($) |
| $C_{intake,ds}$ | Draw solution intake capital cost ($) |
| $C_{intake,fs}$ | Feed solution intake capital cost ($) |
| $C_m$ | Capital cost of membrane module ($) |

| | |
|---|---|
| $C_{m,O\&M}$ | Annual cost of membrane module ($) |
| $C_{ml}$ | Total membrane replacement cost ($) |
| $C_{outfall,bs}$ | Brackish solution outfall capital cost ($) |
| $C_{O\&M}$ | O&M cost (million dollars per year) |
| $E_{osmotic}$ | Osmotic energy per unit volume of fresh water (kWh/m$^3$) |
| $E_{f,fs}$ | Energy consumption of feed solution pre-treatment (MWh) |
| $E_{f,ds}$ | Energy consumption of draw solution pre-treatment (MWh) |
| $E_{i,ds}$ | Energy consumption of intake draw solution (MWh) |
| $E_{i,fs}$ | Energy consumption of intake feed solution (MWh) |
| $E_{loss}$ | Energy loss (MWh) |
| $E_{gen,loss}$ | Energy loss in generators (MWh) |
| $E_{o,bs}$ | Energy consumption of discharging brackish solution (MWh) |
| $E_{m,ds}$ | Energy consumption of membrane module draw solution (MWh) |
| $E_{m,fs}$ | Energy consumption of membrane module feed solution (MWh) |
| $E_{net}$ | Net annual energy production (MWh) |
| $E_{production}$ | Annual energy production (MWh) |
| $E_{turb,loss}$ | Energy loss in turbines (MWh) |
| $J_w$ | Water flux (m$^3$/m$^2 \cdot$ s) |
| $k$ | External concentration polarization mass transfer coefficient (m/s) |
| $K$ | Internal concentration polarization mass transfer coefficient (m/s) |
| $m_{life}$ | Membrane lifetime (years) |
| $n$ | Investment period (years) |
| $P$ | Hydraulic pressure (kPa) |
| $Q_{bs}$ | Flow rate of the brackish solution (m$^3$/s) |
| $Q_{ds}$ | Flow rate of the draw solution (m$^3$/s) |
| $Q_{fs}$ | Flow rate of the feed solution (m$^3$/s) |
| $y$ | Annual time step |

## References


[1] A. Achilli, T. Y. Cath, A. E. Childress, Power generation with pressure retarded osmosis: An experimental and theoretical investigation, Journal of Membrane Science 343 (1-2) (2009) 42–52. doi:10.1016/j.memsci.2009.07.006.
URL http://linkinghub.elsevier.com/retrieve/pii/S0376738809005134

[2] Q. She, X. Jin, C. Y. Tang, Osmotic power production from salinity gradient resource by pressure retarded osmosis: Effects of operating conditions and reverse solute diffusion, Journal of Membrane Science 401-402 (2012) 262–273. doi:10.1016/j.memsci.2012.02.014.
URL http://linkinghub.elsevier.com/retrieve/pii/S037673881200110X

[3] T. T. Tran, C. Bianchi, K. Park, A. D. Smith, Design of housing and mesh spacer supports for salinity gradient hydroelectric power generation using pressure retarded osmosis, in: Technologies for Sustainability (SusTech), 2015 IEEE Conference, 2015, pp. 141–147. doi:10.1109/SusTech.2015.7314337.

[4] K. L. Hickenbottom, J. Vanneste, M. Elimelech, T. Y. Cath, Assessing the current state of commercially available membranes and spacers for energy production with pressure retarded osmosis, Desalination-doi:http://dx.doi.org/10.1016/j.desal.2015.09.029.
URL http://www.sciencedirect.com/science/article/pii/S0011916415300904

[5] G. Han, S. Zhang, X. Li, T. S. Chung, Progress in pressure retarded osmosis (PRO) membranes for osmotic power generation, Progress in Polymer Science 51 (2014) 1–27. doi:10.1016/j.progpolymsci.2015.04.005.
URL http://www.sciencedirect.com/science/article/pii/S0079670015000519 http://linkinghub.elsevier.com/retrieve/pii/S0079670015000519

[6] G. Han, S. Zhang, X. Li, T.-S. S. Chung, High performance thin film composite pressure retarded osmosis (PRO) membranes for renewable salinity-gradient energy generation, Journal of Membrane Science 440 (2013) 108–121. doi:10.1016/j.memsci.2013.04.001.
URL http://linkinghub.elsevier.com/retrieve/pii/S0376738813002810 http://www.sciencedirect.com/science/article/pii/S0376738813002810

[7] Y. Cui, X. Y. Liu, T. S. Chung, Enhanced osmotic energy generation from salinity gradients by modifying thin film composite membranes, Chemical Engineering Journal 242 (2014) 195–203. doi:10.1016/j.cej.2013.12.078.
URL http://www.sciencedirect.com/science/article/pii/S1385894713016598

[8] F. Helfer, C. Lemckert, Y. G. Anissimov, Osmotic power with Pressure Retarded Osmosis: Theory, performance and trends – A review, Journal of Membrane Science 453 (2014) 337–358. doi:10.1016/j.memsci.2013.10.053.
URL http://linkinghub.elsevier.com/retrieve/pii/S037673881300865X

[9] Y. C. Kim, M. Elimelech, Potential of osmotic power generation by pressure retarded osmosis using seawater as feed solution: Analysis and experiments, Journal of Membrane Science 429 (2013) 330–337. doi:10.1016/j.memsci.2012.11.039.
URL http://dx.doi.org/10.1016/j.memsci.2012.11.039

[10] D. W. Stephens, Changes in lake levels, salinity and the biological community of Great Salt Lake (Utah, USA), 1847?1987, Hydrobiologia 197 (1) (1990) 139–146. doi:10.1007/BF00026946.
URL https://pubs.er.usgs.gov/publication/70016259

[11] J. R. McCutcheon, M. Elimelech, Influence of membrane support layer hydrophobicity on water flux in osmotically driven membrane processes, Journal of Membrane Science 318 (1-2) (2008) 458–466. doi:10.1016/j.memsci.2008.03.021.
URL http://www.sciencedirect.com/science/article/pii/S0376738808002238

[12] K. L. Lee, R. W. Baker, H. K. Lonsdale, Membranes for power generation by pressure-retarded osmosis, Journal of Membrane Science 8 (2) (1981) 141–171. doi:10.1016/S0376-7388(00)82088-8.
URL http://www.sciencedirect.com/science/article/pii/S0376738800820888

[13] N. Y. Yip, M. Elimelech, Thermodynamic and energy efficiency analysis of power generation from natural salinity gradients by pressure retarded osmosis, Environmental Science and Technology 46 (9) (2012) 5230–5239. arXiv:arXiv:1408.1149, doi:10.1021/es300060m.

[14] G. O'Toole, L. Jones, C. Coutinho, C. Hayes, M. Napoles, A. Achilli, River-to-sea pressure retarded osmosis: Resource utilization in a full-scale facility, Desalination 389 (2016) 39–51. doi:10.1016/j.desal.2016.01.012.
URL http://dx.doi.org/10.1016/j.desal.2016.01.012

[15] J. L. Prante, J. a. Ruskowitz, A. E. Childress, A. Achilli, RO-PRO desalination: An integrated low-energy approach to seawater desalination, Applied Energy 120 (2014) 104–114. doi:10.1016/j.apenergy.2014.01.013.
URL http://www.sciencedirect.com/science/article/pii/S0306261914000324 http://linkinghub.elsevier.com/retrieve/pii/S0306261914000324

[16] R. Kleiterp, The feasibility of a commercial osmotic power plant.
URL http://repository.tudelft.nl/view/ir/uuid:fbaa8d2f-3c01-45e3-8473-9a2ccd2b9a67/

[17] K. Nijmeijer, S. Metz, Sustainable Water for the Future: Water Recycling versus Desalination, Vol. 2 of Sustainability Science and Engineering, Elsevier, 2010. doi:10.1016/S1871-2711(09)00205-0.
URL http://www.sciencedirect.com/science/article/pii/S1871271109002050

[18] A. Naghiloo, M. Abbaspour, B. Mohammadi-Ivatloo, K. Bakhtari, Modeling and design of a 25MW osmotic power plant (PRO) on Bahmanshir River of Iran, Renewable Energy 78 (November 2009) (2015) 51–59. doi:10.1016/j.renene.2014.12.067.
URL http://dx.doi.org/10.1016/j.renene.2014.12.067

[19] S. Loeb, F. Van Hessen, D. Shahaf, Production of energy from concentrated brines by pressure-retarded osmosis, Journal of Membrane Science 1 (1976) 249–269. doi:10.1016/S0376-7388(00)82271-1.
URL http://www.sciencedirect.com/science/article/pii/S0376738800822577 http://www.sciencedirect.com/science/article/pii/S0376738800822711

[20] S. Loeb, F. V. Hessen, D. Shahaf, Production of Energy From Concentrated Brines By Pres- Sure-Retarded Osmosis Ii. Experimental Results and Projected Energy Costs, Journal of Membmne Sctence 1 (1976) 249–269. doi:10.1016/S0376-7388(00)82271-1.

[21] G. D. Mehta, S. Loeb, Performance of permasep B-9 and B-10 membranes in various osmotic regions and at high osmotic pressures, Journal of Membrane Science 4 (C) (1978) 335–349. doi:10.1016/S0376-7388(00)83312-8.

[22] S. Chou, R. Wang, L. Shi, Q. She, C. Tang, A. G. Fane, Thin-film composite hollow fiber membranes for pressure retarded osmosis (PRO) process with high power density, Journal of Membrane Science 389 (2012) 25–33. doi:10.1016/j.memsci.2011.10.002.
URL http://linkinghub.elsevier.com/retrieve/pii/S037673881100737X

[23] N. Y. Yip, A. Tiraferri, W. A. Phillip, J. D. Schiffman, L. A. Hoover, Y. C. Kim, M. Elimelech, Thin-film composite pressure retarded osmosis membranes for sustainable power generation from salinity gradients, Environmental Science and Technology 45 (10) (2011) 4360–4369. doi:10.1021/es104325z.

[24] W. A. Phillip, J. D. Schiffman, M. Elimelech, High Performance Thin-Film Membrane, Environmental Science & Technology 44 (10) (2010) 3812–3818.

[25] B. D. Barnes, W. A. Wurtsbaugh, The effects of salinity on plankton and benthic communities in the Great Salt Lake, Utah, USA: a microcosm experiment, Canadian Journal of Fisheries and Aquatic Sciences 72 (6) (2015) 807–817. doi:10.1139/cjfas-2014-0396.
URL http://www.nrcresearchpress.com/doi/abs/10.1139/cjfas-2014-0396#.VxBjXjArJaR

[26] J. S. White, S. E. Null, D. G. Tarboton, Modeled changes to Great Salt Lake salinity from railroad causeway alternation, Ph.D. thesis, Utah State University (2014).
URL http://www.deq.utah.gov/locations/G/greatsaltlake/railroadcauseway

[27] EIA, U.S. Energy Information Administration - EIA - Independent Statistics and Analysis.
URL http://www.eia.gov/state/?sid=UT#tabs-4

[28] Pump Efficiencies.
URL http://www.pump-manufacturers.com/

[29] T. Al-Sarkal, H. A. Arafat, Ultrafiltration versus sedimentation-based pretreatment in Fujairah-1 RO plant: Environmental impact study, Desalination 317 (2013) 55–66. doi:10.1016/j.desal.2013.02.019.
URL http://www.sciencedirect.com/science/article/pii/S0011916413000933

[30] K. Gerstandt, K. V. Peinemann, S. E. Skilhagen, T. Thorsen, T. Holt, Membrane processes in energy supply for an osmotic power plant, Desalination 224 (1-3) (2008) 64–70. doi:10.1016/j.desal.2007.02.080.
URL http://www.sciencedirect.com/science/article/pii/S0011916408000325

[31] Microfiltration/Ultrafiltration.
URL http://www.waterrf.org/Pages/Index3.aspx

[32] J.-M. Laîné, D. Vial, P. Moulart, Status after 10 years of operation — overview of UF technology today, Desalination 131 (1-3) (2000) 17–25. doi:10.1016/S0011-9164(00)90002-X.
URL http://www.sciencedirect.com/science/article/pii/S001191640090002X

[33] S. Sundaramoorthy, G. Srinivasan, D. Murthy, An analytical model for spiral wound reverse osmosis membrane modules: Part I — Model development and parameter estimation, Desalination 280 (1-3) (2011) 403–411. doi:10.1016/j.desal.2011.03.047.
URL http://www.sciencedirect.com/science/article/pii/S0011916411002657

[34] S. E. Skilhagen, J. E. Dugstad, R. J. Aaberg, Osmotic power - power production based on the osmotic pressure difference between waters with varying salt gradients, Desalination 220 (1-3) (2008) 476–482. doi:10.1016/j.desal.2007.02.045.
URL http://www.sciencedirect.com/science/article/pii/S0011916407006467
http://linkinghub.elsevier.com/retrieve/pii/S0011916407006467

[35] R. J. Aaberg, Osmotic Power: A new and powerful renewable energy source?, Refocus 4 (6) (2003) 48–50. doi:10.1016/S1471-0846(04)00045-9.

[36] Desalination: A National Perspective, The National Academies Press, Washington, D.C. doi:10.17226/12184.

[37] S. Loeb, Large-scale power production by pressure-retarded osmosis, using river water and sea water passing through spiral modules, Desalination 143 (2) (2002) 115–122. doi:10.1016/S0011-9164(02)00233-3.

[38] S. E. Skilhagen, Osmotic Power: a new, renewable source of energy, Proceedings of the 3rd Annual European Renewable Energy Makerts.

[39] G. A. Aggidis, E. Luchinskaya, R. Rothschild, D. C. Howard, The costs of small-scale hydro power production: Impact on the development of existing potential, Renewable Energy 35 (12) (2010) 2632–2638. doi:10.1016/j.renene.2010.04.008.
URL http://dx.doi.org/10.1016/j.renene.2010.04.008

[40] Residential Price Comparison (2015).
URL https://www.rockymountainpower.net/about/rar/rpc.html

[41] Energy Information Administration, Levelized Cost and Levelized Avoided Cost of New Generation Resources in the Annual Energy Outlook 2016, US Energy Information Administration (August) (2016) 1–20.
URL https://www.eia.gov/outlooks/aeo/pdf/electricity_generation.pdf

[42] Great Salt Lake, https://www.google.com/earth/ (2016).

Table 1: Flow rate of intake and outfall solutions.

| Feed Solution $Q_{fs}$ ($m^3/s$) | Draw Solution $Q_{ds}$ ($m^3/s$) | Brackish Solution $Q_{bs}$ ($m^3/s$) |
|---|---|---|
| 1.54 | 3.08 | 4.47 |

Table 2: Net annual energy production.

| $\dot{W}_{net}$ (MW) | $E_{osmotic}$ ($kWh/m^3$) | $E_{production}$ (MWh) | $E_{loss}$ (MWh) | $E_{net}$ (MWh) |
|---|---|---|---|---|
| 25 | 4.5 | 197,100 | 42,851 | 154,249 |

Table 3: Break down of energy loss and consumption

| Subsystems | Energy Loss (MWh) | Percentage (%) |
|---|---|---|
| Intake and Outfall | -10,578 | -5.37% |
| Solution Pre-treatment | -1,094 | -0.56% |
| Membrane Module | -1,614 | -0.82% |
| Electro-mechanical System | -29,565 | -15.00% |
| Total Energy Loss | -42,850 | -21.74% |
| Potential Energy Production | +197,100 | +100% |
| Net Energy Production | +154,249 | +78.26% |

Table 4: Break down of capital cost.

| Subsystems | Capital Cost (million dollars) | Percentage (%) |
|---|---|---|
| Intake and Outfall | 76.6 | 32.12% |
| Solution Pre-treatment | 109.9 | 46.23% |
| Membrane Module | 37.5 | 15.78% |
| Electro-mechanical System | 6.8 | 2.87% |
| Miscellaneous | 7.2 | 3.00% |
| Total Capital Cost | 238.0 | 100% |

Table 5: Cost of the power plant.

| Total Capital Cost (million dollars) | Annual O&M Cost (million dollars per year) | Membrane Replacement Cost (million dollars per membrane lifetime) |
|---|---|---|
| 238.0 | 33.5 | 18.8 |

Table 6: Comparison of LCOE of osmotic power at the Great Salt Lake to LCOE of other renewable power generation technologies.

| Plant Type | Average Total System LCOE ($/kWh) [41] |
|---|---|
| Geothermal | 0.0450 |
| Wind | 0.0645 |
| Hydroelectric | 0.0678 |
| Solar PV | 0.0847 |
| Biomass | 0.0961 |
| Wind – Offshore | 0.1581 |
| **Osmotic Power** | **0.2025** |
| Solar Thermal | 0.2359 |

Table 7: Sensitivity analysis on energy performance of the power plant.

| Parameter | Symbol | Design Value | Min. Value | Max. Value |
|---|---|---|---|---|
| Turbine Efficiency (%) | $\eta_{turb}$ | 90 | 85 | 95 |
| Generator Efficiency (%) | $\eta_{gen}$ | 95 | 90 | 98 |
| Pump Efficiency (%) | $\eta_{pump}$ | 75 | 70 | 80 |

Table 8: Sensitivity analysis on cost of the power plant.

| Parameter | Symbol | Design Value | Min. Value | Max. Value |
|---|---|---|---|---|
| Membrane Performance (W/m$^2$) | $W$ | 5 | 1 | 15 |
| Pre-treatment Unit Price ($/m$^3$) | $C_{unit,f}$ | 275 | 250 | 300 |
| Membrane Module Unit Price ($/m$^2$) | $C_{unit,m}$ | 7.5 | 5 | 10 |
| Membrane Lifetime (year) | $m_{life}$ | 5 | 5 | 10 |

Table 9: Sensitivity analysis on economics of the power plant.

| Parameter | Symbol | Design Value | Min. Value | Max. Value |
|---|---|---|---|---|
| Investment Period (year) | $n$ | 40 | 30 | 50 |
| Discount Rate (%) | $r$ | 2 | 0 | 5 |

Table 10: Results of sensitivity analysis.

| Parameters | Range | $\Delta C_{total}$ (million dollars) | $\Delta E_{net}$ (MWh) | $\Delta$LCOE ($/kWh) |
|---|---|---|---|---|
| $\eta_{turb}$ (%) | 85 - 95 | — | +19,710 | -0.0260 |
| $\eta_{gen}$ (%) | 90 - 98 | — | +15,768 | -0.0213 |
| $\eta_{pump}$ (%) | 70 - 80 | — | +1,633 | -0.0021 |
| $W$ (W/m$^2$) | 1 - 15 | -187.6 | — | -0.1047 |
| $C_{unit,f}$ ($/m$^3$) | 250 - 300 | +20.6 | — | +0.0033 |
| $C_{unit,m}$ ($/m$^2$) | 5 - 10 | +25.8 | — | +0.0147 |
| $m_{life}$ (year) | 5 - 10 | -75.0 | — | -0.0084 |
| $n$ (year) | 30 - 50 | — | — | -0.0504 |
| $r$ (%) | 0 - 5 | — | — | -0.1246 |

Table 11: Results of the improved design.

| Capital Cost (million dollars) | Net Energy Production (MWh) | LCOE ($/kWh) |
|---|---|---|
| 197.2 | 166,837 | 0.1034 |

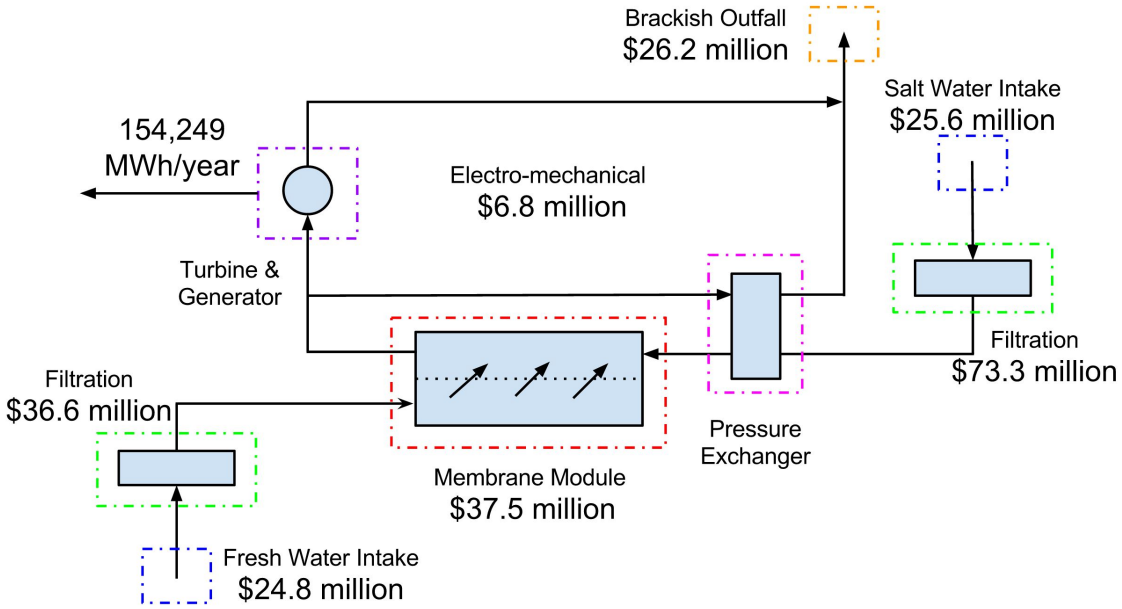


Figure 1: Graphical abstract.

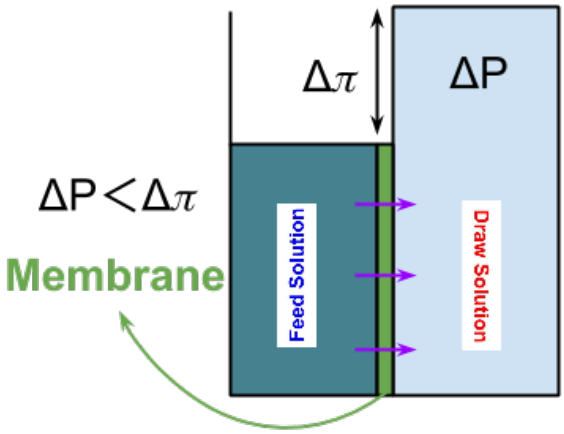


Figure 2: Illustration of PRO process.

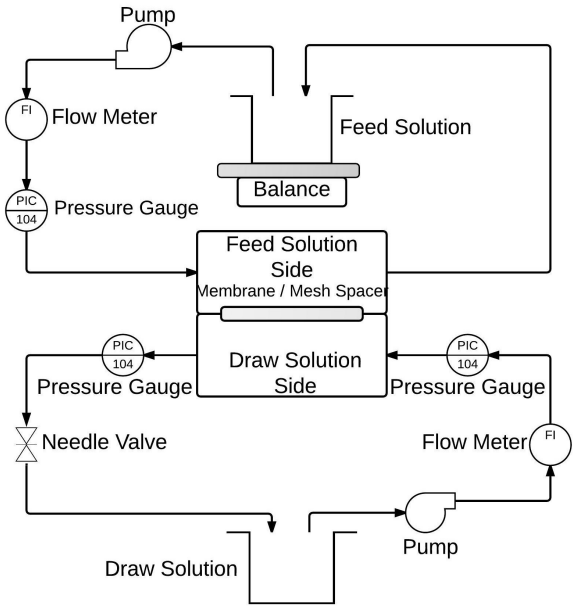


Figure 3: Bench-scale PRO schematic [3].

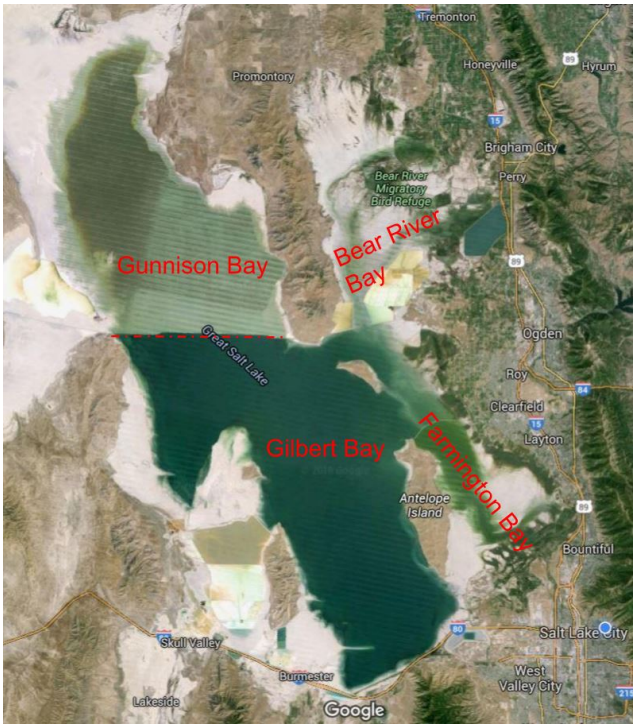


Figure 4: Bird's eye view of the Great Salt Lake from Google Earth [42].

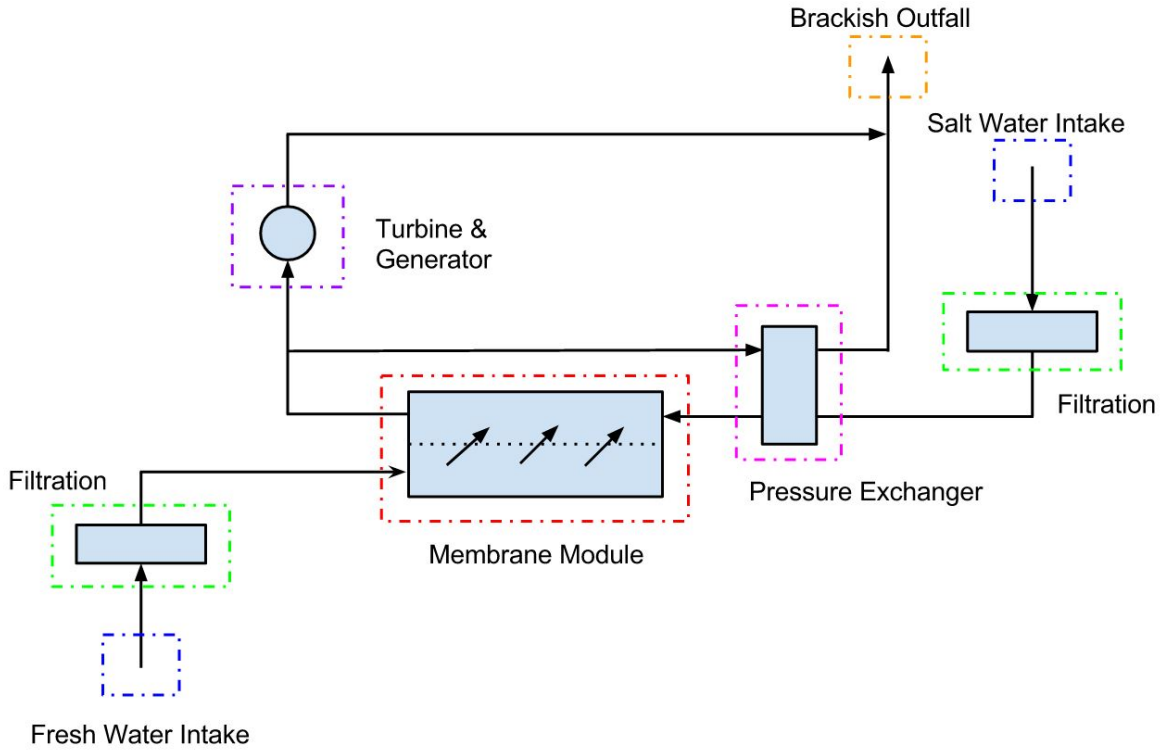


Figure 5: System diagram of large-scale PRO system.

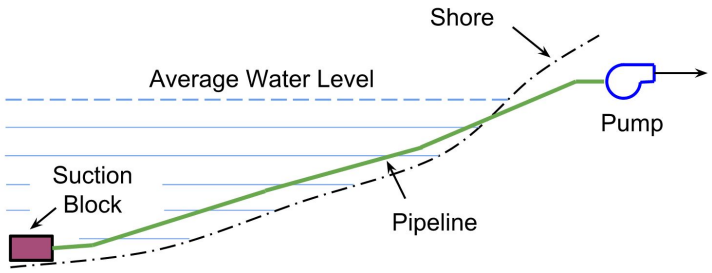


Figure 6: Schematic diagram of the deep-water intake system.

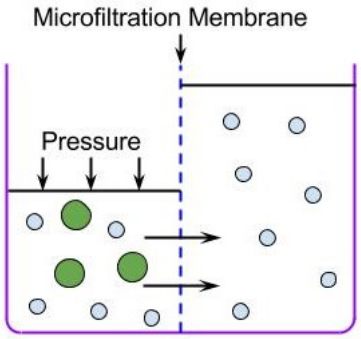


Figure 7: Schematic diagram of the microfiltration process.

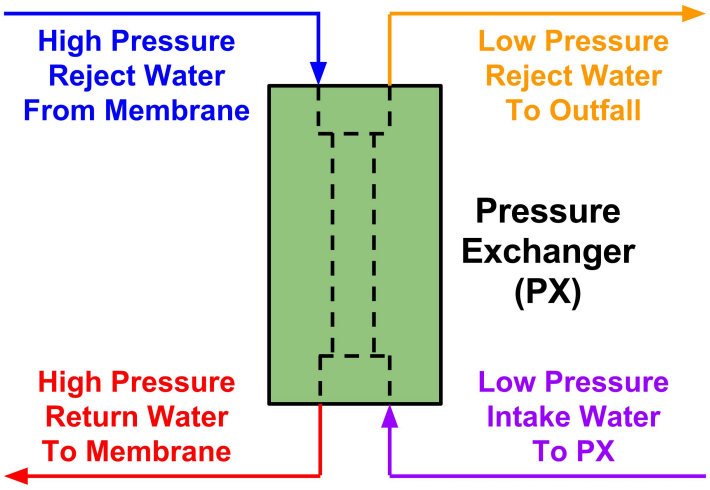


Figure 8: Pressure exchanger operation.

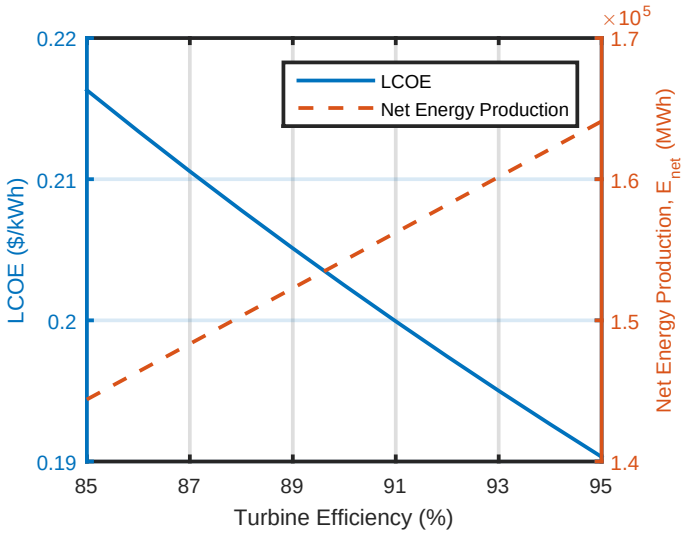


Figure 9: Sensitivity analysis on turbine efficiency.

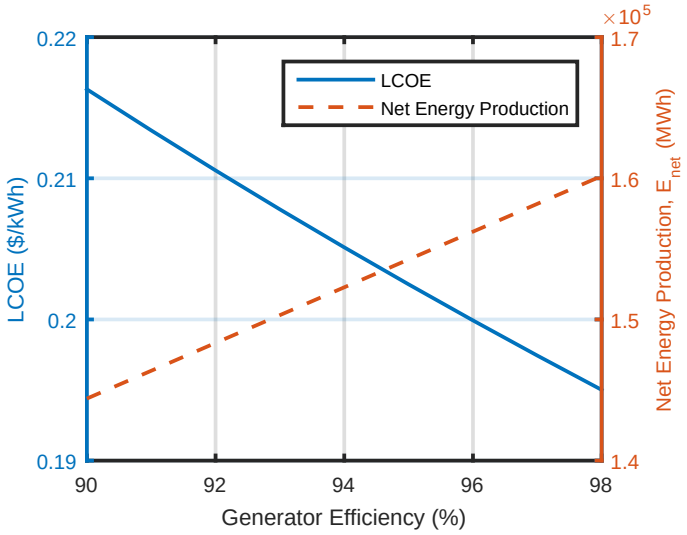


Figure 10: Sensitivity analysis on generator efficiency.

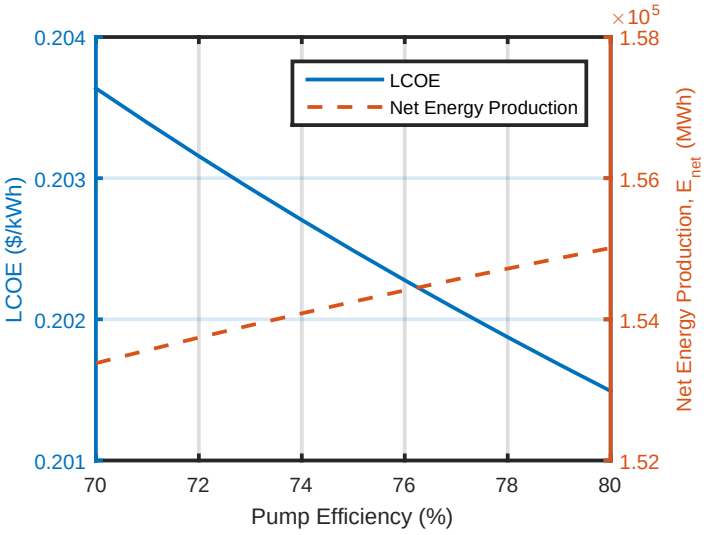


Figure 11: Sensitivity analysis on pump efficiency.

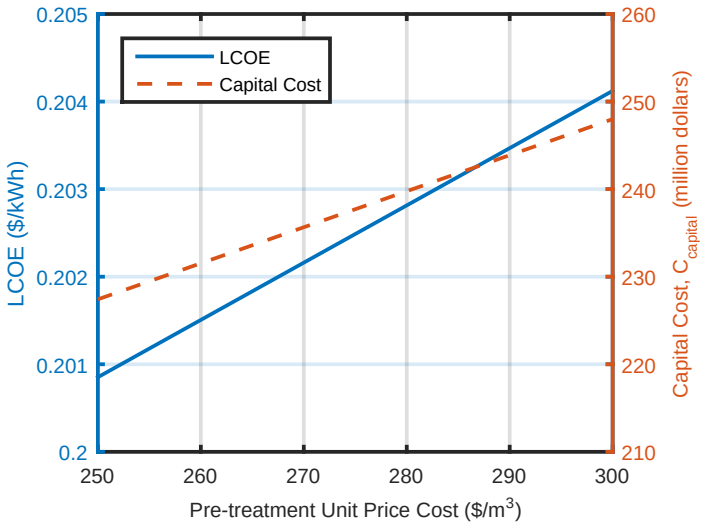


Figure 12: Sensitivity analysis on solution pre-treatment unit price cost.

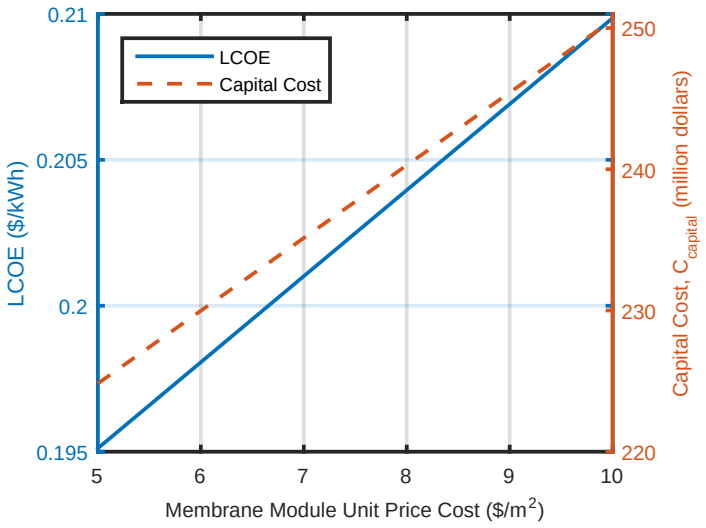


Figure 13: Sensitivity analysis on membrane module unit price cost.

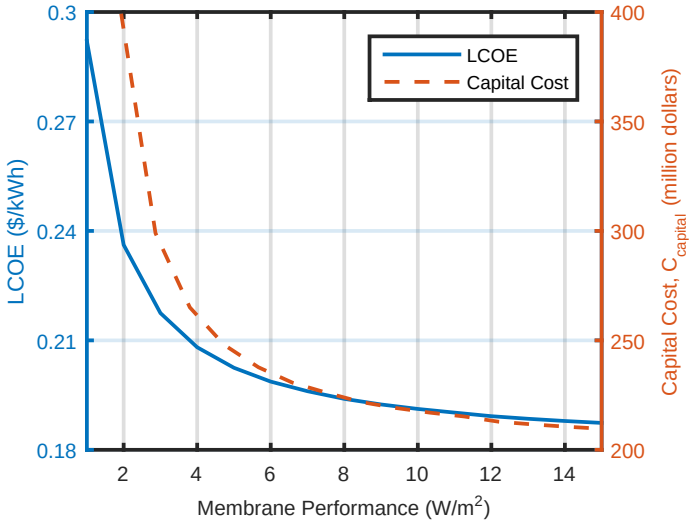


Figure 14: Sensitivity analysis on membrane performance.

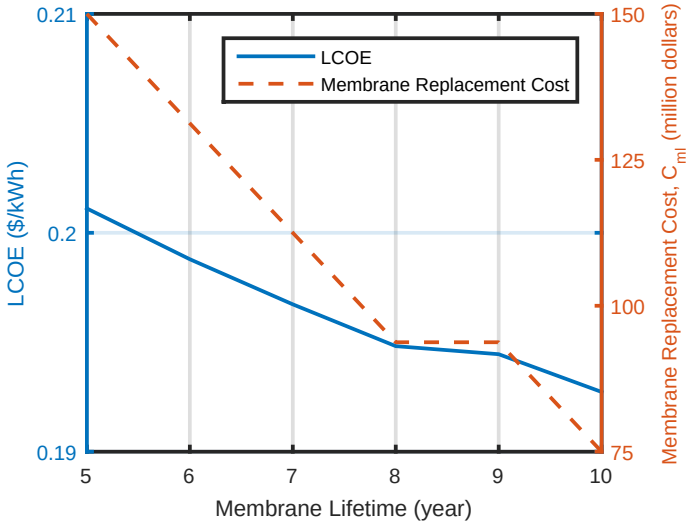


Figure 15: Sensitivity analysis on membrane lifetime.

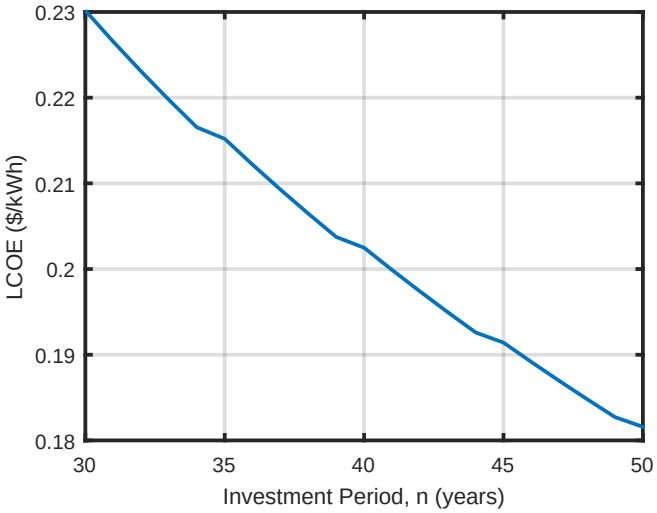


Figure 16: Sensitivity analysis on investment period.

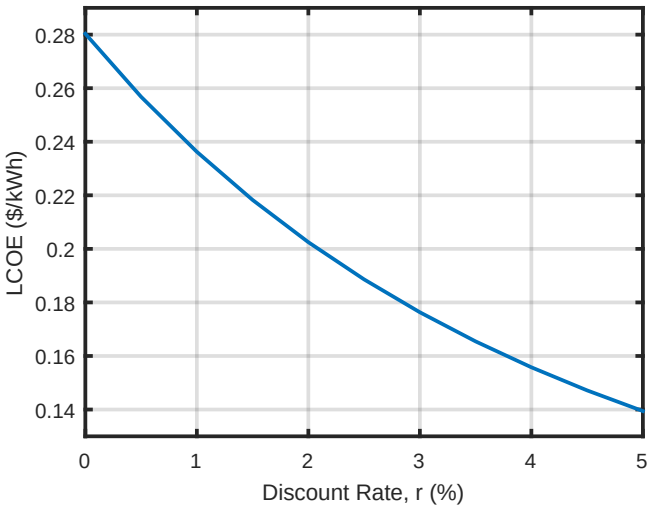


Figure 17: Sensitivity analysis on discount rate.